

# Development and Application of Distributed Multilayer On-line Monitoring System for High Voltage Vacuum Circuit Breaker

Mei Fei<sup>†</sup>, Mei Jun<sup>\*</sup>, Zheng Jianyong<sup>\*</sup> and Wang Yiping<sup>\*</sup>

**Abstract** – On-line monitoring system is important for high voltage vacuum circuit breakers (HVCBs) in operation condition assessment and fault diagnosis. A distributed multilayer system with client/server architecture is developed on rated voltage 10kV HVCB with spring operating mechanism. It can collect data when HVCB switches, calculate the necessary parameters, show the operation conditions and provide abundant information for fault diagnosis. Ensemble empirical mode decomposition (EEMD) is used to detect the singular point which is regarded as the contact moment. This method has been applied to on-line monitoring system successfully and its satisfactory effect has been proved through experiments. SVM and FCM are both effective methods for fault diagnosis. A combinative algorithm is designed to judge the faults of HVCB's operating mechanism. The system's precision and stability are confirmed by field tests.

**Keywords:** Distributed system, Fault diagnosis, On-line monitoring system, Parameters calculation, Vacuum circuit breaker

## 1. Introduction

High Voltage Circuit Breakers (HVCBs) that are used to configure a power system as needed, control the load flow and disconnect any fault parts of the system are important primary equipment in power system [1]. Since the operation conditions of HVCBs are directly related to the safety and reliability of the power system, the online monitoring system for HVCBs is essential [2-5]. However, for HVCBs, existing monitoring system based on single microprocessor cannot meet the requirements of huge data's rapid transmission and real-time processing [6]. Moreover, independent monitoring devices are difficult to accomplish data exchange. As a result, diagnosis accuracy becomes lower relatively owing to the lack of support from remote expert system. In this paper, we design and develop a distributed multilayer system with client/server architecture. In this system, client computers collect available data, set up historical database, calculate the necessary parameters and show the current operation status. Server computer regularly receives data messages including mechanical parameters, operating mechanism status, temperature, humidity and other information from client computers, which are helpful to the judgment of operation condition and analysis of potential faults.

Among all the mechanical parameters, contact moment is the most important one that must be acquired firstly in the process of calculation. However, it is troublesome to

obtain in the on-line manner. Much progress on this problem has been achieved in the researches, such as zero point of contacts velocity judgment method [7], appearance point of closing coil current judgment method [8] and analysis method of vibration signal based on the wavelet packets extraction algorithm and short-time energy [9]. Nevertheless, owing to different rated voltages, the types and structures of operating mechanisms are distinguished. Therefore, the means above are not suitable for the monitoring system we developed due to the reasons below:

- Zero point of velocity lags the contact moment, for the reason that after the closing time, a short period of time is needed for the velocity to drop to zero.
- When the closing coil current appears, it just means the beginning of the closing, a period of time is needed for the breaker to close completely.
- Though detecting the contact moment through vibration signals has higher accuracy, it needs extra three signal channels. Furthermore, due to small space of the three phases of vacuum circuit breaker, coupled with the electromagnetic environment interference, aliasing will easily appears in signals, which makes it harder for us to distinguish.

To solve the problem, we design a method based on singularity detection to gain the contact moment, which can make full use of the sampling displacement data to calculate mechanical parameters. Traditionally, a large number of researches on singularity detection are based on wavelet analysis [10-13]. However, both selection of wavelet basis function and the number of decomposition level determines the effect of signal processing. In this

<sup>†</sup> Corresponding Author: School of Electrical Engineering, Southeast University, China.(meifei@seu.edu.cn)

<sup>\*</sup> School of Electrical Engineering, Southeast University, China. ({mei\_jun, jy\_zheng}@seu.edu.cn, yp\_wang2007@126.com)

Received: June 5, 2012; Accepted: February 4, 2013

condition, it is hard for us to get the optimal effect.

Empirical mode decomposition (EMD) proposed by N.E.Huang is the method suitable to process nonlinear and non-stationary signals [14]. Benefit from its self-adaption, it has been widely used in engineering in recent years since it overcomes the shortcomings of wavelet transformation [15-17]. In addition, EMD is an appropriate selection for singularity detection since several intrinsic mode functions (IMF) that contain the characteristic information with different scales can be obtained through decomposition in EMD. However, mode mixing problem brought by EMD probably leads to the difficulty of characteristic extraction. Thus, Wu and Huang proposed a modified method called ensemble empirical mode decomposition (EEMD) [18]. Through adding white noise to original signal, multiple decomposition and averaging IMFs in different levels, mode mixing can be eliminated effectively. In this paper, EEMD is adopted to detect closing moment, subsequently, mechanical parameters can be obtained. The effectiveness of this method is proved in experiments.

Fault diagnosis plays an important role in HVCBs' on-line monitoring system; it also represents the main development of intelligent circuit breakers. The accuracy of diagnosis depends on precise disposal of sampling signals as well as flexible design of intelligent algorithms. The diagnosis algorithms that are currently available mostly rely on analysis and disposal of control coil current or vibration signals [19-20]. For intelligent algorithm, learning machines or neural networks are firstly used to train fault dataset [21-22], test samples are then input into the classifier. Consequently, fault types can be obtained. In this paper, closing coil current is chosen as the sampling signal, which covers the advantages of steadiness, smaller interference, obvious characteristic and easy acquisition. Then a fault diagnosis system based on FCM (Fuzzy Clustering Method) and SVM (Support Vector Machine) is designed. The diagnosis results are in accordance with reality.

## 2. Overall Structure of the System

At present, distributed on-line monitoring technology has been widely used in many fields. The work pattern is the combination of distributed collection and centralized processing of sampling data. However, in the field of HVCB, most on-line monitoring devices work in an independent way. On one hand, deficiency of centralized management makes a large number of HVCBs in intelligent substations unable to form efficient integrated system. On the other hand, without support from experience of remote expert system, accuracy of condition assessment and fault diagnosis is lower. Therefore, we design the monitoring system based on client/server architecture as shown in Fig. 1.

This system is divided into five levels obviously. Each

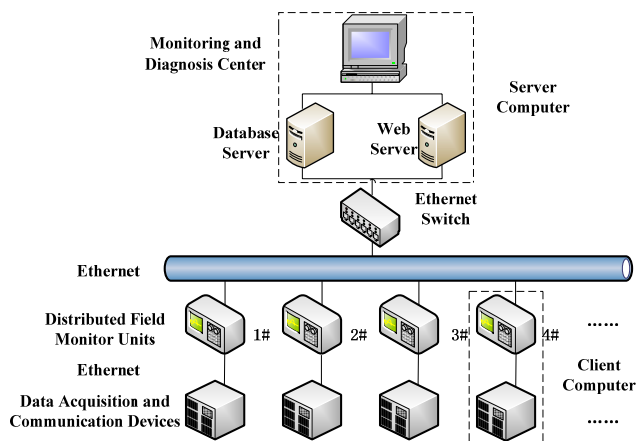


Fig. 1. Topological structure of distributed on-line monitoring system

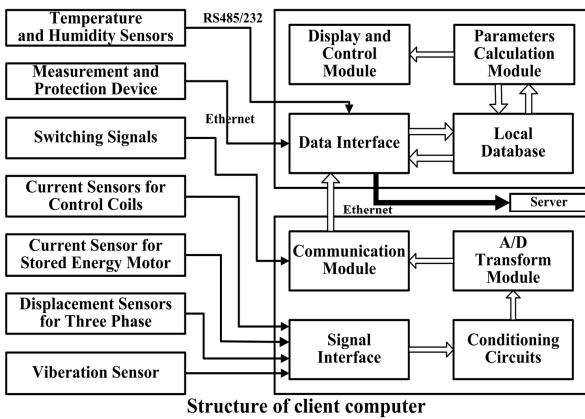
level has its own function:

- Data acquisition level: collects data and transmits them to the next level.
- Local monitoring level: shows current status, builds local database, calculates parameters, sends data message, and receives orders from servers.
- Ethernet communication level: exchanges and transmits data.
- Server level: gathers switching parameters and status information of each HVCB, provides database and WEB service.
- Monitoring and diagnosis level: diagnoses faults and assesses conditions according to the information from the database server.

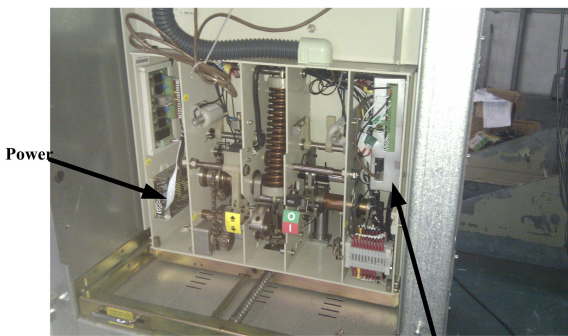
## 3. Hardware and Software of Client Computer

### 3.1 Hardware structure

Each client computer is installed on switchgear including data acquisition device and local monitoring unit which are connected with each other by Ethernet. In this paper, we develop a client computer on VMB5-12 HVCB adopting the construct of host computer plus slave computer with master-slave processing model. Each slave computer (data acquisition and communication device) is the embedded system based on ARM (Advanced RISC Machines) and FPGA (Field-Programmable Gate Array). In each slave computer, FPGA is used to collect the sampling data from A/D and ARM is the core of communication since FPGA has abundant I/O interfaces and rapid parallel processing capacity while ARM has powerful communication ability. This dual core architecture plays an important role in the system. Therefore, multi-channel real-time data sampling with high speed can be realized. Host computer (local monitoring unit) is composed of single board computer

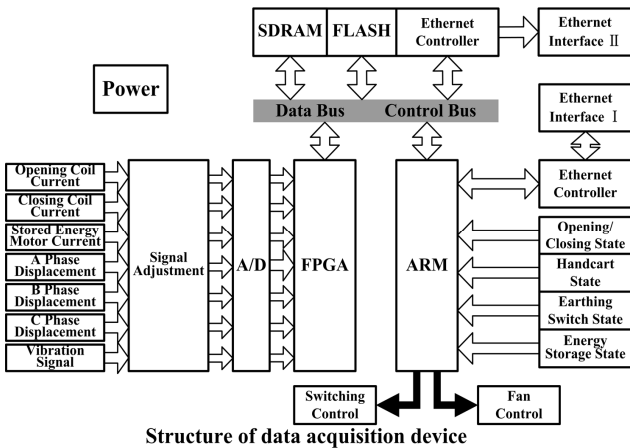


Structure of client computer



Installation of data acquisition device on HVCB

(a)



Structure of data acquisition device



FPGA+ARM acquisition board

(b)

Fig. 2. Client computer of on-line monitoring system

(SBC), led touch screen, hard disk and power. It can receive and save sampling data from slave computer, calculate the parameters, show the results with graphs and tables as well as communicate with servers through Ethernet. The structures of client computer, data acquisition and communication device are shown in Figs. 2(a) and (b).

The sampling data has two parts. One is analog signal and the other is switching signal. Analog signals include opening/closing coil current, stored energy motor current, three-phase displacement and vibration signal. Switching signals include opening/closing state, handcart state, earthing switch state and energy storage state. Moreover, it can receive control signals from local monitoring unit. Besides, extended channels are reserved in order to accept more signals in the future.

### 3.2 Coordinating work model of dual-core

There exist two communication modes between FPGA and ARM: parallel communication and serial communication. In order to meet the high requirement of real-time property, we adopt serial communication taking its high efficiency into account. After getting data from A/D, FPGA sends an IRQ3 interrupt signal to ARM. Then ARM dispatches chip selection and reads signals to FPGA immediately when it detects IRQ3. Subsequently, ARM begins to read the data from FPGA and saves them in SDRAM. At the same time, ARM checks the switching signals and arranges all of these data in data message. Finally, ARM sends the data message through Ethernet. This work model is shown in Fig. 3.

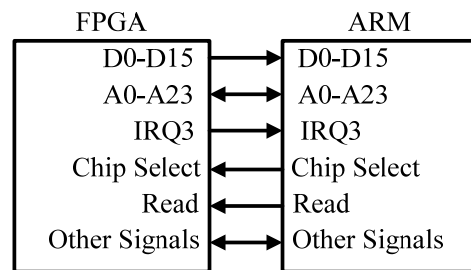
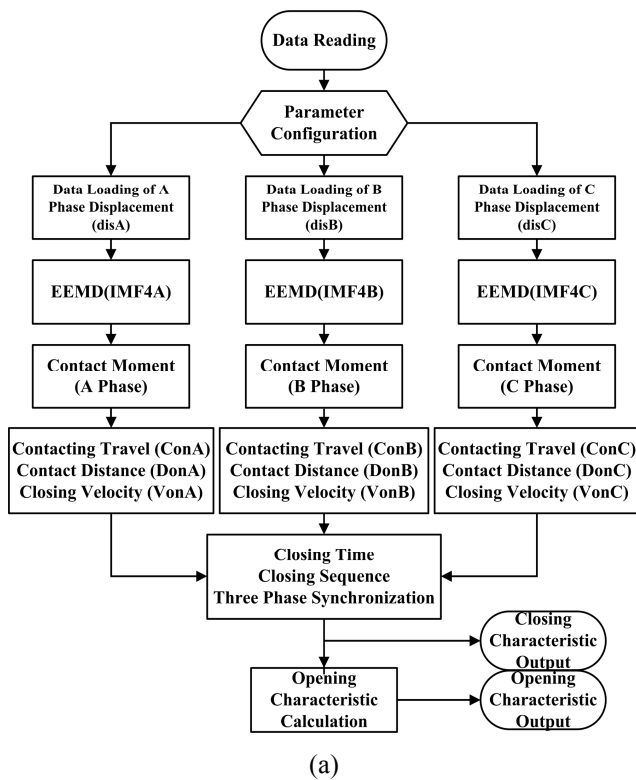


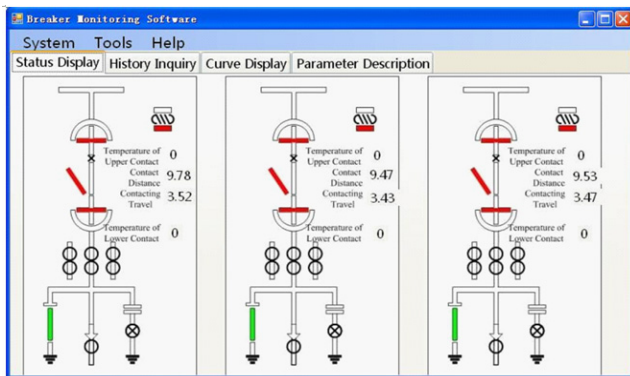
Fig. 3. Coordinating work model of ARM and FPGA

### 3.3 Software structure

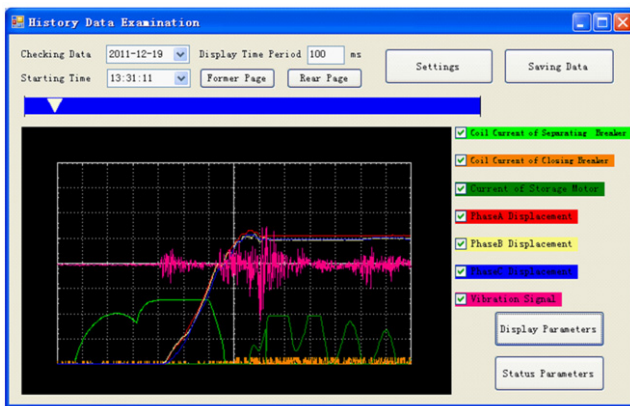
In this paper, the on-line monitoring software is developed and run on the local monitoring unit which can display the current status, waveforms of sampling signals in real time. Moreover, it can save data when HVCBs operate, query historical records anytime, show the parameters after calculation and send data messages to servers. The mechanical parameters calculation flow, main interface and wave recording picture are shown in Figs. 4(a) and (b). The algorithm is realized by MATLAB. All the programs are compiled into COM components that can be invoked by software.



(a)



Main interface



Wave recording

(b)

Fig. 4. Software parameter calculation flow and operation main interface

#### 4. EMD and EEMD Method

The basic hypothesis of EMD is that all the signals are composed of a series of IMFs. IMF has two characteristics: (a) in the whole data set, the number of extrema and the number of zero crossings must either be equal or differ at most by one; (b) at any point, the mean value of the envelope defined by the local maxima and the envelope defined by the local minima is zero [14]. EMD is used to decompose sampling signal  $X(t)$  into several IMFs  $C_i(t)$  and the margin  $r_n(t)$  as follows:

$$X(t) = \sum_{i=1}^n C_i(t) + r_n(t) \quad (1)$$

The decomposition flow of EMD is shown in Fig. 5.

- Top envelope  $e_{\max}(t)$  and bottom envelope  $e_{\min}(t)$  are obtained through cubic spline interpolation using local extrema of  $X(t)$ .
- Mean value  $m_i(t)$  is the average of  $e_{\max}(t)$  and  $e_{\min}(t)$ .

$$m_i(t) = (e_{\max}(t) + e_{\min}(t)) / 2 \quad (2)$$

- Terminal conditions of  $h_i(t)$  are the IMF characteristics above.
- Finally, if margin  $r_n(t)$  is a monotone function or its amplitude differences are less than the threshold we defined, decomposition finishes. Generally, standard deviation  $S_d$  is used to be the threshold, and  $S_d$  is defined in the range from 0.2 to 0.3.

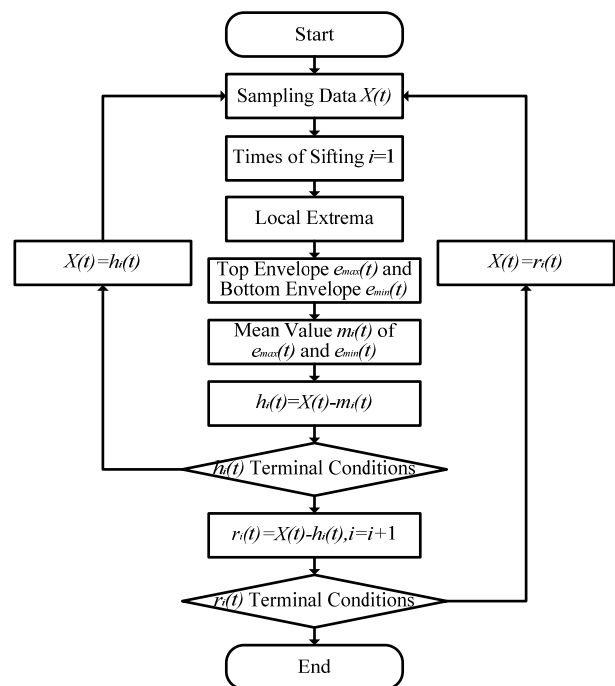


Fig. 5. EMD decomposition flow



$$S_d = \sum_{t=1}^T \frac{|h_{k-1}(t) - h_k(t)|^2}{h_{k-1}^2(t)} \quad (3)$$

$$\overline{C_j} = \sum_{m=1}^M C_{j,m} / M \quad (6)$$

In this paper, we use the termination criterion proposed by GRilling, which includes three parameters:  $\theta_1$ ,  $\theta_2$  and  $\alpha$ . Evaluation function  $\sigma(t)$  is defined as:

$$\sigma(t) = \left| \frac{e_{\max(k)}(t) + e_{\min(k)}(t)}{e_{\max(k)}(t) - e_{\min(k)}(t)} \right| \quad (4)$$

Decomposition will continue until  $\sigma(t) < \theta_1$  for some prescribed fraction  $(1-\alpha)$  of the total duration, while  $\sigma(t) < \theta_2$  for the remaining fraction [23].

EEMD is suitable for singularity detection owing to the overcoming of mode mixing brought by EMD. Essentially, EEMD is the repeated EMD by adding Gaussian white noise in each decomposition. Taking advantage of uniform distribution statistical characteristics of Gaussian white noise in frequency domain, sampling signal contained noise will continue in different scales. Therefore, the resistance of IMFs to mode mixing is enhanced. Characteristics will be highlighted more obviously. The flow of EEMD is shown in Fig. 6.

- Before EMD, the signal  $X_m(t)$  to be decomposed is the sampling signal  $X(t)$  added with random white noise  $n_m(t)$ .

$$X_m(t) = X(t) + kn_m(t) \quad (5)$$

$k$  is the amplitude coefficient.

- Each sifting will produce a series of IMFs  $C_{j,m}(t)$ ,  $j = 1, 2, 3, \dots, p$ .
- The final IMFs  $\overline{C_j}$  is the average of  $C_{j,m}(t)$ .

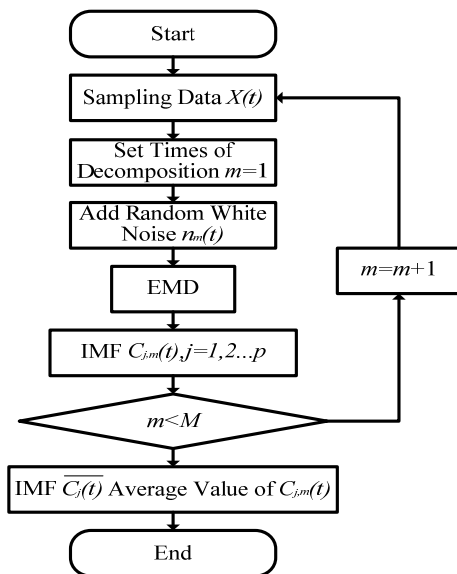


Fig. 6. EEMD decomposition flow

We can get the optimal results through adjusting the parameters  $M$  and  $k$ . The decomposition flow of EEMD is shown in Fig. 6.

## 5. Application of EMD and EEMD Methods in Mechanical Parameters Calculation

### 5.1 Analysis of displacement curve of closing process

The typical displacement waveform of VCB with spring operating mechanism collected by displacement sensors is shown in Fig. 7. Then we can find out four obvious stages in the closing process.

- Stage T1: Circuit breaker remains opening and its displacement is approximately zero.
- Stage T2: Closing coil begin to be active (B point) and moving contacts start to move towards static contacts with relatively stable speed.
- Stage T3: Moving contacts and static contacts touch with each other. However, moving contacts will not stop until contacting travel generated with lower speed.
- Stage T4: Contacts stop and circuit breaker becomes closed.

At the closing moment of contact, the acceleration of moving contact will drop to zero instantly due to the reaction force. Therefore, an abrupt change will occur at this point in displacement curve (C point). Then we can get its position and regard it as the closing moment.

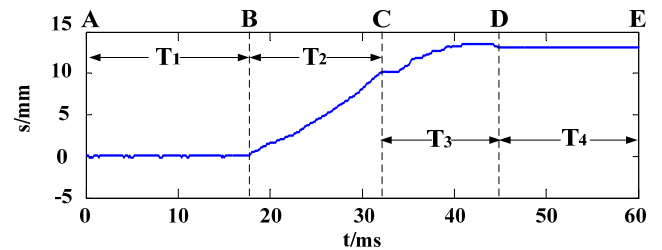


Fig. 7. Typical waveform of closing trip displacement signal of vacuum circuit breaker

### 5.2 Application and analysis of EMD

Mode mixing is a phenomenon that there are different characteristic time scales in one IMF or similar characteristic time scales in different IMFs. It appears frequently in the IMFs when we use EMD to process signals with singularity. In this paper, EMD is applied to process closing displacement signal of HVCB. Fig. 8 shows the waveform of the results

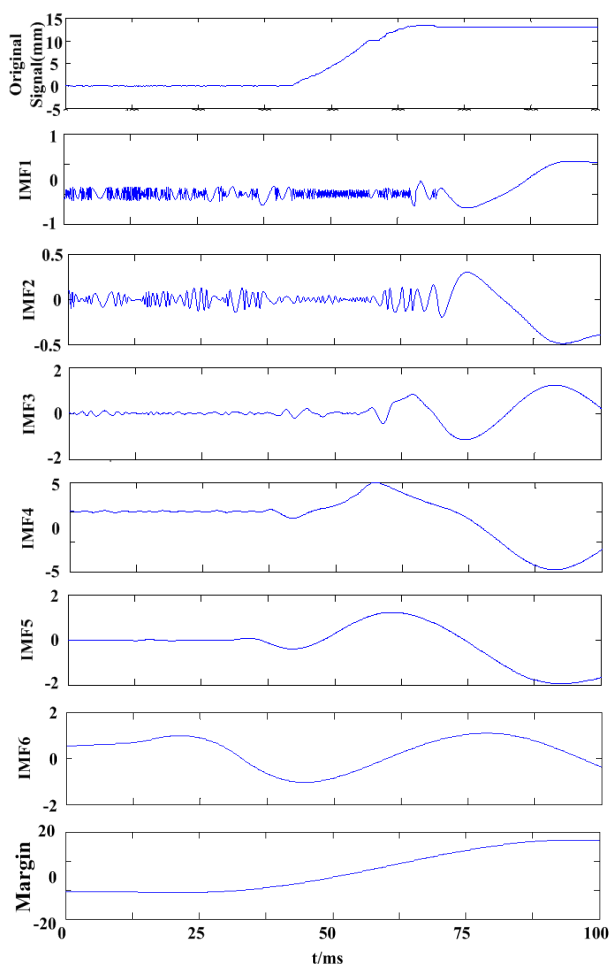


Fig. 8. Results of EMD decomposition

including original signal, IMF1-IMF6 and margin. From it, we can see that there are serious mode mixings in IMF1 and IMF2. Due to some characteristic events (start, contact and stop) in the displacement signal, local extrema are abnormal distributed. Subsequently, cubic spline interpolation will produce some distortions. Therefore, mode mixing appears.

### 5.3 Application and analysis of EEMD

Singular points of displacement signals are difficult to detect due to the mode mixing caused by EMD. Therefore, this paper uses EEMD ultimately to process these sampling signals choosing parameters  $M = 100$  and  $k = 0.1$ . Fig. 9 shows the results of EEMD using the same original signal as above. From the figure we can see that EEMD can eliminate mode mixing efficiently and the effect is satisfactory. Moreover, there exist maximum peak in IMF4 which corresponds to contact moment in original signal. Resulted from the huge reaction force, there is maximum variation at contact moment which can be easily obtained through EEMD.

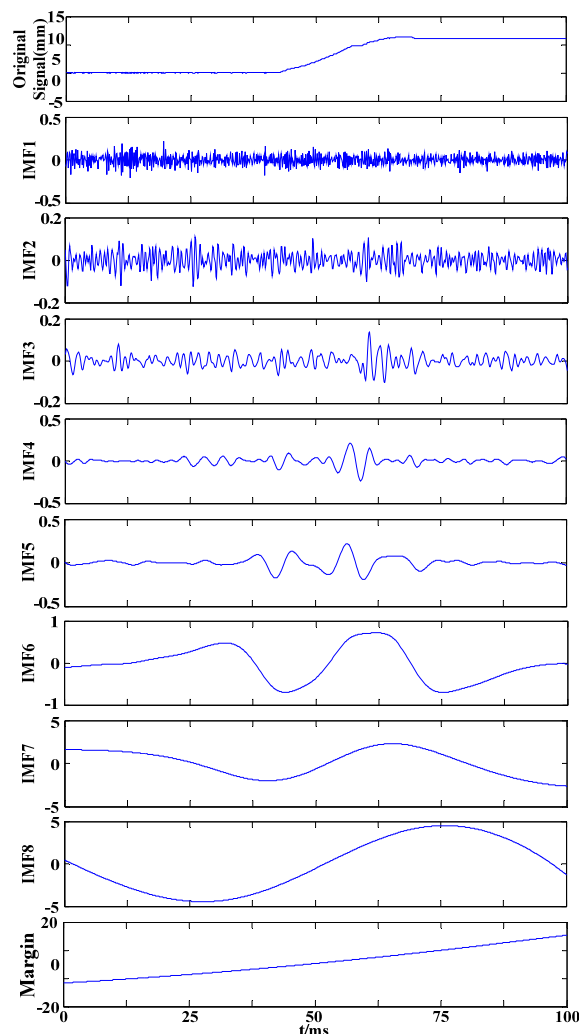


Fig. 9. Results of EEMD decomposition

## 6. Experiment and Analysis

The proposed on-line monitoring system has been installed on HVCBs rated 10kV with spring operation mechanism. In order to test the accuracy and reliability of the on-line monitoring system, 10 groups of data containing three-phase displacement are collected and mechanical parameters are calculated. The results are compared with that of circuit breaker's characteristics tester SA100. Fig. 10 shows the two results of original displacement signals and IMF4 components using singularity detection method based on EEMD.

Contact travel is defined as the distance of moving contacts between the contact moment point and the stopping point. Its measurement accuracy can directly represent the calculation accuracy of the mechanical parameters. Table 1 shows the comparison results. The contact travel of experimental prototype is adjusted to 3.5 mm.

The experimental results show that all the errors are lower than 4%. Moreover, the standard deviations of three-

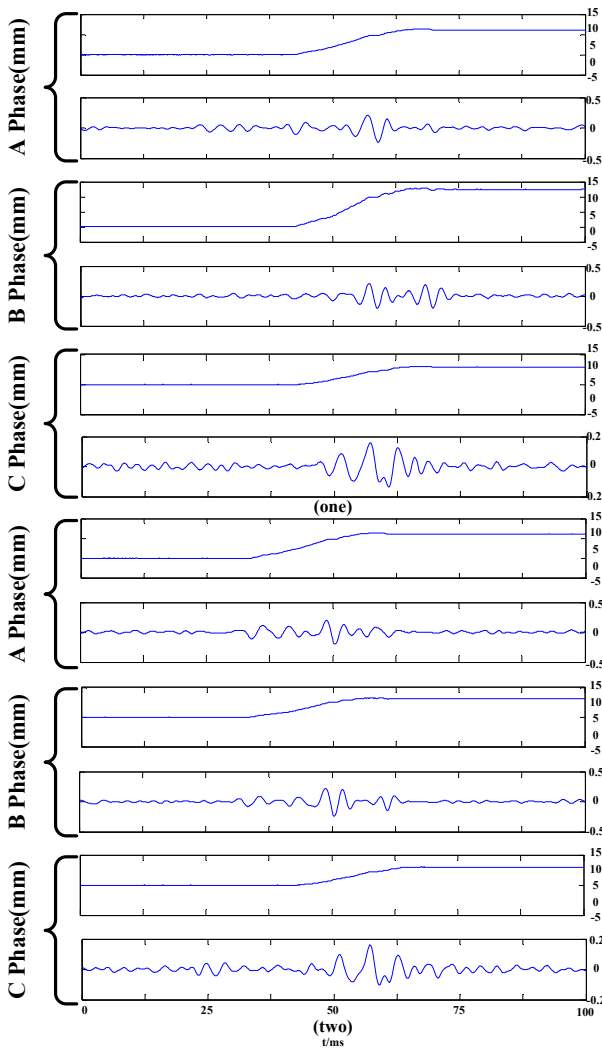


Fig. 10. Waveform of original displacement signals and IMF5 components

Table 1. Experiment data of circuit breaker's contact travel

Number	A phase (mm)	Error (%)	B phase (mm)	Error (%)	C phase (mm)	Error (%)
1	3.5804	2.30	3.4755	0.70	3.5591	1.69
2	3.4106	2.55	3.4319	1.95	3.5589	1.68
3	3.6160	3.31	3.4971	0.08	3.5556	1.59
4	3.5702	2.01	3.4267	2.09	3.5556	1.59
5	3.4047	2.72	3.4361	1.83	3.5606	1.73
6	3.6079	3.08	3.4313	1.96	3.5561	1.60
7	3.6166	3.33	3.4258	2.12	3.5578	1.65
8	3.6092	3.12	3.4357	1.84	3.5556	1.59
9	3.5973	2.78	3.4705	0.84	3.5556	1.59
10	3.5822	2.35	3.4801	0.57	3.4589	1.17

phase are respectively 0.0816, 0.0266 and 0.0311. Therefore, we can consider that the accuracy and stability of the EEMD judgment method is high enough to meet the demands for on-line monitoring system.

The data in Table 2 is typical mechanical parameters of HVCB from the field tests of on-line monitoring system.

Table 2. Experiment data of HVCB's on-line monitoring system

type	A phase	B phase	C phase
Contact Distance(mm)	3.58	3.48	3.56
Contacting Travel(mm)	9.52	9.52	9.24
Closing Velocity(m/s)	0.69	0.66	0.72
Closing Time(ms)	36.2		
Closing Synchronization(ms)	0.68		
Opening Velocity(m/s)	1.08	1.21	1.13
Opening Time(ms)	22.4		
Opening Synchronization(ms)	0.18		

## 7. Design of Fault Diagnosis System

### 7.1 Closing coil current and eigenvalue extraction

On-line monitoring system acquires HVCBs' closing coil current signals by means of Hall current sensor (Model: HNC-03SY). Fig. 11 shows the typical current curve of closing coil under normal operation with DC power supply.

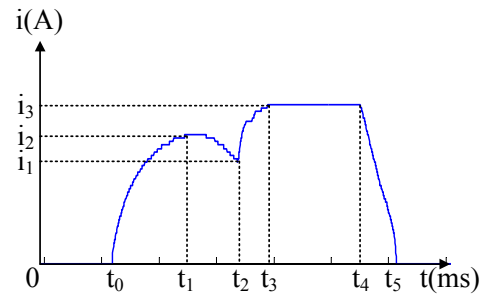


Fig. 11. Typical curve of closing coil current

In Fig. 11, current curve is divided into five periods:

- $t_0$ -  $t_1$ : At  $t_0$  moment, the appearance of closing signal causes the coil to energize; the current starts to rise until  $t_1$  when the iron core begins to move.
- $t_1$ -  $t_2$ : The moving of iron core results in current drop until  $t_2$  when the iron core contacts the buckle.
- $t_2$ -  $t_3$ : The iron core stops due to the prevention of buckle, current rises again.
- $t_3$ -  $t_4$ : The current reaches a steady state.
- $t_4$ -  $t_5$ : The iron core moves following the separation of buckle, which makes the current drops to zero at  $t_5$  moment.

Closing coil current is relatively steady and convenient to extract eigenvalues. In our fault diagnosis system, eight parameters (include current parameters  $\{i_1, i_2, i_3\}$  and time parameters  $\{t_1, t_2, t_3, t_4, t_5\}$  in Fig. 11) are utilized as eigenvalues to create characteristic space, simultaneously assume  $t_0=0$  as reference point to calculate time parameters.

### 7.2 The process of fault diagnosis algorithm

The diagnosis system we designed combines FCM and

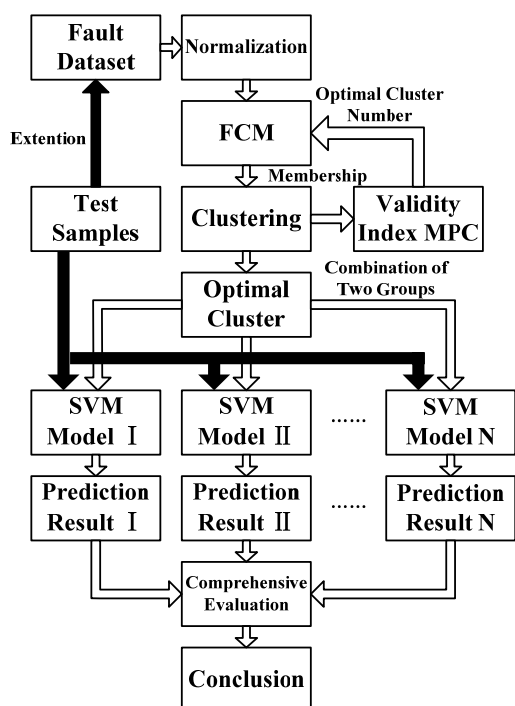


Fig. 12. Diagnosis algorithm flow

SVM to dispose fault data. FCM is a well-known clustering algorithm, which coincides with the faults' characteristics of ambiguity and uncertainty better compared with hard clustering algorithm. Therefore, FCM is widely used in areas of classifiers, pattern recognition and fault diagnosis, etc. As an alternative algorithm for neural network, SVM owns obvious advantages in solving high dimensional, small sample and nonlinear problems. FCM is adopted to classify fault dataset. After that SVM creates several prediction models using categorical data. Consequently, test samples will be inputted into these models for the final diagnosis results. Fig. 12 shows the process of this algorithm.

The process is shown in details as follows:

- Step 1: Normalize fault dataset on the basis of extremum standardization formula:

$$x_{ik}'' = \frac{x_{ik}'' - x_{k \min}''}{x_{k \max}'' - x_{k \min}''} \quad (7)$$

$x_{ik}''$  represents the parameter in row  $i$  and column  $k$  of fault dataset.  $x_{k \max}''$  and  $x_{k \min}''$  respectively represents the maximum and minimum data in column  $k$ .

- Step 2: FCM is utilized to cluster fault dataset into  $C$  classes and membership degree matrix is calculated.
- Step 3: The cluster validity is measured by MPC, the maximum of which represents optimal cluster number.

$$MPC = 1 - \frac{C}{1-C} \left( 1 - \frac{1}{N} \sum_{c=1}^C \sum_{i=1}^N u_{ic} \right) \quad (8)$$

$C$  represents cluster number,  $N$  represents sample number,  $u_{ic}$  represents membership degree matrix.

- Step 4: SVM training devices can be created by each two groups of optimal clusters, after which we can obtain  $C \times (C-1)/2$  prediction models.
- Test samples are inputted into the prediction models respectively. Subsequently, the type of fault can be judged.

### 7.3 Test and analysis

In order to verify the effectiveness of the above-mentioned fault diagnosis algorithm, we collect 50 sets of fault data while 40 sets of them are taken as training samples. As shown in Table 3, these 40 sets are original samples of FCM and SVM model. The remaining 10 sets are test samples.

Input these 40 sets into FCM classifier. Number of

Table 3. Training samples of fault dataset

No	$t_1$	$t_2$	$t_3$	$t_4$	$t_5$	$i_1$	$i_2$	$i_3$
1	10.2	17.56	21.72	34.68	39.68	0.99	0.78	1.22
2	10.24	17.6	21.72	34.64	39.72	0.99	0.77	1.21
3	10.28	17.64	21.76	34.64	39.76	0.77	0.67	1.03
4	10.24	17.6	21.76	34.68	39.76	0.78	0.69	1.05
⋮	⋮	⋮	⋮	⋮	⋮	⋮	⋮	⋮
39	10.24	19.32	21.68	34.64	39.64	0.98	0.78	1.24
40	10.24	19.2	21.8	34.72	39.68	0.97	0.78	1.22

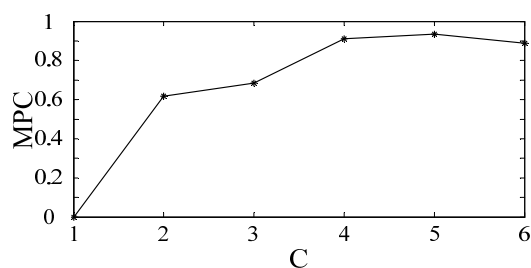

 Fig. 13. Trend of MPC with different values of  $C$ 

Table 4. Optimal categorical dataset

	$t_1$	$t_2$	$t_3$	$t_4$	$t_5$	$i_1$	$i_2$	$i_3$
F1	10.2	17.56	21.72	34.68	39.68	0.99	0.78	1.22
	10.24	17.6	21.72	34.64	39.72	0.99	0.77	1.21
	⋮	⋮	⋮	⋮	⋮	⋮	⋮	⋮
F2	10.28	17.64	21.76	34.64	39.76	0.77	0.67	1.03
	10.24	17.6	21.76	34.68	39.76	0.78	0.69	1.05
	⋮	⋮	⋮	⋮	⋮	⋮	⋮	⋮
F3	10.76	21.68	26.64	37.84	43.48	1.01	0.79	1.24
	10.84	21.84	26.84	37.96	43.88	1.01	0.8	1.25
	⋮	⋮	⋮	⋮	⋮	⋮	⋮	⋮
F4	10.2	17.56	21.72	37.68	42.68	0.99	0.78	1.22
	10.28	17.52	21.84	37.64	42.72	0.98	0.78	1.22
	⋮	⋮	⋮	⋮	⋮	⋮	⋮	⋮
F5	10.28	19.32	21.64	34.6	39.64	0.98	0.78	1.22
	10.24	19.2	21.68	34.64	39.6	0.98	0.79	1.23
	⋮	⋮	⋮	⋮	⋮	⋮	⋮	⋮



**Table 5.** Test samples

No	$t_1$	$t_2$	$t_3$	$t_4$	$t_5$	$i_1$	$i_2$	$i_3$
1	10.16	17.56	21.68	34.68	39.72	0.99	0.79	1.21
2	10.24	17.64	21.68	34.6	39.72	0.98	0.77	1.2
3	10.32	17.64	21.8	34.64	39.8	0.76	0.67	1
4	10.32	17.48	21.76	34.76	39.8	0.78	0.69	1.06
5	10.88	21.8	26.76	38.04	43.84	1.02	0.81	1.24
6	11.12	22.08	27.08	38.16	44.24	1.03	0.82	1.24
7	10.24	17.68	21.76	37.88	43.04	0.99	0.81	1.23
8	10.16	17.44	21.76	37.68	42.72	0.99	0.8	1.24
9	10.32	19.44	21.64	34.64	39.72	0.98	0.79	1.22
10	10.28	18.32	21.76	34.6	39.72	0.99	0.8	1.23

clusters  $C$  is defined as a natural number range from 2 to  $C_{max}$  (the maximum of  $C_{max}$  is  $\sqrt{N}$ ). The values of MPC will be changed with different values of  $C$ . Fig. 13 shows the trend of MPC.

From Fig. 13 we can see that MPC reaches maximum when  $C=5$ , this means the best cluster number of fault dataset is 5. Then re-cluster fault dataset and label every fault types. Optimal categorical dataset is shown in Table 4.

10 SVM prediction models can be created by combination of arbitrary two groups of data in optimal categorical dataset. Consequently, 10 test samples are inputted into these prediction models respectively. Then we can obtain 100 prediction results. Integration of these results is needed for the diagnosis conclusions at last. Table 5 shows 10 groups of test samples while we can see diagnostic results in Table 6.

Each SVM prediction model will produce a predictive result for every test sample. Then the result with highest occurrence number will be regarded as the final diagnostic conclusion. From Table 6 we can see that judgments of test samples using FCM and SVM method are exactly the same with the fault type it belongs to. Therefore, we can draw a conclusion that this algorithm is reliable.

### 8. Conclusion

On-line monitoring system for HVCBs is an essential component in integrated automation system of smart substation. In this paper, some preliminary researches have

been accomplished. Especially, we also design a distributed multilayer structure and develop the client computer based on the proposed method. Through field tests, the calculation accuracy and stability of the proposed system have been proved. Moreover, the flexibility and reliability of the whole system are guaranteed. In the next period, fault diagnosis and pattern recognition modules will be developed further to support remote expert system. With powerful data processing and communication ability, on-line monitoring system will be widely applied to power system in the future.

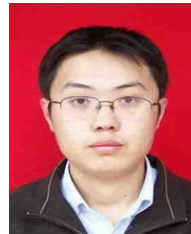
### References

- [1] Knezev M, Djekic Z and Kezunovic M, "Automated Circuit Breaker Monitoring," in *IEEE Power Engineering Society General Meeting*, Tampa, USA, June 2007.
- [2] Wang Xiaohua, Rong Mingzhe, Wu Yi and Liu Dingxin, "Method of quick fault diagnosis and new knowledge obtainment for high voltage circuit breaker expert system," *Proceedings of the CSEE*, Vol.27, No.12, pp.95-99, 2007.
- [3] Strachan SM, McArthur SDJ, Stephen B, McDonald JR and Campbell A, "Providing decision support for the condition-based maintenance of circuit breakers through data mining of trip coil current signatures," *IEEE Trans on Power Delivery*, Vol. 22, No. 1, pp. 178-186, 2007.
- [4] Zhang Xiang, Zhang Jiaosuo, Gockenbach Ernst and Borsi Hossein, "Life Management of SF(6) Circuit Breakers based on Monitoring and Diagnosis," *IEEE Electrical Insulation Magazine*, Vol. 25, No. 3, pp. 21-29, 2009.
- [5] Stephen B, Strachan SM, McArthur SDJ, McDonald JR and Hamilton K, "Design of trip current monitoring system for circuit breaker condition assessment," *IET Generation Transmission & Distribution*, Vol. 1, No. 1, pp. 89-95, 2007.
- [6] Jian Huang, Peilei Rao, Xiaoguang Hu and Jin Xiao, "Research of on-line monitoring system of the condition of circuit breaker based on ARM and

**Table 6.** Prediction results and conclusions

No	Type	SVM1	SVM2	SVM3	SVM4	SVM5	SVM6	SVM7	SVM8	SVM9	SVM10	Conclusion
1	F1	F1	F1	F1	F1	F2	F2	F2	F4	F5	F5	F1
2	F1	F1	F1	F1	F1	F2	F2	F2	F4	F5	F5	F1
3	F2	F2	F1	F1	F1	F2	F2	F2	F4	F5	F5	F2
4	F2	F2	F1	F1	F1	F2	F2	F2	F4	F5	F5	F2
5	F3	F2	F3	F4	F5	F3	F4	F5	F3	F3	F4	F3
6	F3	F2	F3	F4	F5	F3	F4	F2	F3	F3	F4	F3
7	F4	F2	F1	F4	F1	F2	F4	F2	F4	F5	F4	F4
8	F4	F2	F1	F4	F1	F2	F4	F2	F4	F5	F4	F4
9	F5	F2	F1	F1	F5	F3	F2	F5	F4	F5	F5	F5
10	F5	F2	F1	F1	F5	F3	F2	F5	F4	F5	F5	F5

- FPGA,” in *IEEE International Conference on Control and Automation*, Christchurch, New Zealand, Dec, 2009.
- [7] Lan Jianjun, Hong Zhiyong, Lin Qingyu and Lun Xianmin, “The Research of Method of High Voltage Circuit Breaker Parameter Monitoring and Life Prediction,” *Journal of Northeast Dianli University*, Vol. 31, No. 1, pp. 57-60, 2011.
- [8] Xiong Xiaofu, Sun Xin, Cai Weixian and Yang yang, “Distributed monitoring system based on DSP and ARM for mechanical characteristic of high voltage,” *Power System Protection and Control*, Vol. 37, No. 6, pp. 64-68, 2009.
- [9] Ma Qiang, Rong Mingzhe, Jia Shenli, “Study of Switching Synchronization of High Voltage Breakers Based on The Wavelet Packets Extraction Algorithm and Short Time Analysis Method,” *Proceedings of the CSEE*, Vol. 25, No. 13, pp. 149-154, 2005.
- [10] Charbkaew N, Suwanasri T, Bunyagul T and Schnettler A, “Vibration signal analysis for condition monitoring of puffer-type high-voltage circuit breakers using wavelet transform,” *IEEJ Transactions on Electrical and Electronic Engineering*, Vol. 7, No. 1, pp. 13-22, 2012.
- [11] Jiang X, Ma ZGJ, “Crack Detection from the Slope of the Mode Shape Using Complex Continuous Wavelet Transform,” *Computer-aided Civil and Infrastructure Engineerin*, Vol. 27, No. 3, pp. 187-201, 2012.
- [12] Zhu Hongjun, Qin Shuren, Peng Liling, “Accurate Detection for Peakvalue Singular Points of the Transient Signal with Wavelet Transforms,” *Chinese Journal of Mechanical Engineering*, Vol. 38, No. 12, pp.10-15, 2002.
- [13] Zhang Feng, Liang Jun, Zhang Li and Yun Zhihao, “Traveling Wave Signal Processing Method for Singularity Detection Based on Singularity Value Decomposition and Wavelet Transform,” *Automation of Electric Power Systems*, Vol. 32, No. 20, pp. 57-60, 2008.
- [14] Huang NE, Shen Z, Long S, et al, “The Empirical Mode Decomposition and the Hilbert Spectrum for Nonlinear and Non-stationary Time Series Analysis,” *Proceedings of the Royal Society of London Series A*, 2008.
- [15] Guo W, Tse PW, Djordjevich A, “Faulty bearing signal recovery from large noise using a hybrid method based on spectral kurtosis and ensemble empirical mode decomposition,” *Measurement*, Vol. 45, No. 5, pp.1308-1322, 2012.
- [16] Yang Xiaoping, Liu Pusen, Zhong Yanru, “Harmonic Detection of Active Power Filter Based on Empirical Mode Decomposition,” *Transactions of China Electrotechnical Society*, Vol. 24, No. 5, pp. 197-202, 2009.
- [17] Jia Rong, Xu Qihui, Tian Lulin, Li Hui and Liu Wei, “Denoising of Partial Discharge Based on Empirical Mode Decomposition and Intrinsic Mode Function Reconstruction,” *Transactions of China Electrotechnical Society*, Vol. 23, No. 1, pp. 13-18, 2008.
- [18] Wu ZH, Huang NE, “Ensemble empirical mode decomposition: a noise assisted data analysis method,” *Advances in Adaptive Data Analysis*, Vol. 1, No. 1, pp. 1-14, 2009.
- [19] Ni Jianjun, Zhang Chuanbiao, Yang Simon X, “An Adaptive Approach Based on KPCA and SVM for Real-Time Fault Diagnosis of HVCBs,” *IEEE Trans on Power Delivery*, Vol. 26, No. 3, pp. 1960-1971, 2011.
- [20] Hoidalen HK, Runde M, “Continuous monitoring of circuit breakers using vibration analysis,” *IEEE Trans on Power Delivery*, Vol. 20, No. 4, pp. 2458-2465, 2005.
- [21] Huang Jian, Hu Xiaoguang, Yang Fan, “Support vector machine with genetic algorithm for machinery fault diagnosis of high voltage circuit breaker,” *Measurement*, Vol. 44, No. 6, pp. 1018-1027, 2011.
- [22] Lü Chao, Yu Honghai, Wang Lixin, “On-line Self-learning Fault Diagnosis for Circuit Breakers Based on Artificial Immune Network,” *Proceedings of the CSEE*, Vol. 29, No. 34, pp. 128-134, 2009.
- [23] G Rilling, P Flandrin and P Gonçalves, “On empirical mode decomposition and its algorithms,” *IEEE-EURASIP Workshop on NSIP*, 2003.



**Mei Fei He** received the B.S. degree in mechanical engineering from the Southeast University (SEU) in 2002, and master's degree in mechanical engineering from SEU in 2005. He is a doctoral candidate in electrical engineering in SEU now. His research interests are smart grid, on-line monitoring technology and signal processing.



**Mei Jun He** received the B.S. degree in radio engineering from the Chongqing University in 1994, and the M.S. and Ph.D. degrees in electrical engineering from the Southeast University, Nanjing, China, in 2001 and 2006. He is now an associate professor in the School of Electrical Engineering, Southeast University. From 2011 to 2012, he was a visiting scholar in University of Tennessee, Knoxville, TN. His interests are electric power converters for distributed energy sources, FACTS and power quality control.



**Zheng Jianyong** He was born in China, in 1966. He received his B.S., M.S., and Ph.D. in the School of Electrical Engineering from Southeast University, Jiangsu, China in 1988, 1991, and 1999, respectively. He is now a Full Professor in the School of Electrical Engineering, Southeast University. His research interests are in the fields of

the application of power electronics in power system and renewable energy technology.



**Wang Yiping** She received the B.S. degree in electrical engineering from Jiangsu University. Her research interest is smart grid.